EPJ Web of Conferences **313**, 01003 (2024) https://doi.org/10.1051/epjconf/202431301003
*EC22*

# Nonlinear Landau damping of electron Bernstein waves in MAST-U

*Mads Givskov* Senstius[1,*], *Simon* Freethy[2], *Stefan Kragh* Nielsen[3], and *Michael* Barnes[1]

[1]Rudolf Peierls Centre for Theoretical Physics, University of Oxford, Oxford OX1 3NP, United Kingdom
[2]Culham Centre for Fusion Energy, UKAEA, Abingdon, OX14 3DB, United Kingdom
[3]Department of Physics, Technical University of Denmark, Fysikvej, DK-2800 Kgs. Lyngby, Denmark

**Abstract.** The Mega-Amp Spherical Tokamak Upgrade (MAST-U) is preparing to investigate microwave based current drive using an advanced wave coupling scheme known as O-X-B at high power. The main goal is to assert if this is an efficient method for current drive in the future fusion demonstration power plant STEP. A model for the nonlinear wave-particle interaction nonlinear Landau damping (NLD) is presented. A relativistic, kinetic and electrostatic description is used. For MAST-U, NLD could lead to heating and current drive at the upper hybrid (UH) layer or at the electron cyclotron (EC) resonance of a substantially downshifted daughter wave produced by the wave-particle interactions. It is found that the typical treatment used for nonlinear wave-interactions fails at two critical points in the vicinity of the UH layer.

## 1 Introduction

High power microwaves are commonly applied in magnetically confined fusion devices for electron cyclotron (EC) resonance heating (ECRH) and current drive (ECCD). Whilst ECRH and ECCD have several favorable qualities in a future fusion power plant, ECCD is generally not as efficient at driving current as neutral beam injection (NBI) or lower hybrid current drive. Older microwave experiments indicate that electron Bernstein waves (EBWs) may rival the current drive efficiency of NBI[1]. However, the EBWs are excited from X-mode at the upper hybrid (UH) layer, which is also associated with several nonlinear effects. At high power densities, nonlinear wave interactions may degrade the performance of EBW based current drive and heating.

Two gyrotrons are being installed at the Mega Amp Spherical Tokamak Upgrade (MAST-U) to investigate the viability of EBW operation. If high power EBWs are found to drive current efficiently, the future UK Spherical Tokamak for Energy Production (STEP) demonstration power plant is expected to use EBWs to achieve better performance[2]. In preparation of EBW experiments at MAST-U, fully kinetic particle-in-cell (PIC) simulations have indicated that nonlinear effects may strongly interfere with the linear excitation of EBWs at the UH layer[3]. The previous study focused on the parametric decay instability and stochastic electron heating, and whilst thresholds from the literature for these effects appeared to agree with observations in the simulations, it was not clear that they alone accounted for the suppression of linear excitation of EBWs. Because the UH layer is found between the second and third EC frequency in MAST-U, another nonlinear effect known as nonlinear Landau damping (NLD)[4, 5] is possible. NLD is a nonlinear wave-particle interaction, and in a magnetized fusion plasma, NLD can cause the desired EBWs to interact with the gyrating electrons, transferring energy to them and generating an EBW signal downshifted by the local EC frequency. The effect can also be thought of as nonlinear EC damping or quasi-mode decay. This can lead to electron heating and current drive to occur at positions other than the target EC resonance. Because the impact of NLD depends nonlinearly on the amplitude of the gyrotron beam, it is necessary to understand how NLD affects the power deposition profile in MAST-U.

In this paper, we derive an analytical model of the excitation of a daughter wave downshifted in frequency relative to a gyrotron wave due to NLD in MAST-U. The model is made to fit a geometry like in the 1D PIC simulations in [3]. A number of challenges arise in this geometry. Some are solved with a relativistic description, others cannot easily be solved within the WKB approximation that is typically used to model nonlinear wave interactions.

## 2 The electron Bernstein wave (EBW) and O-X-B

### 2.1 Linear wave behavior

The EBWs are electrostatic waves which are a kinetic phenomenon not captured by the cold plasma fluid model typically used for O- and X-mode waves. The EBWs are carried by the gyrating electrons of the magnetized plasma and exist in frequency bands between the harmonics of the EC frequency. Part of the waves are forward propagating and part of them are backward propagating, typically with a group velocity much smaller than the speed of light. The EBWs are strongly damped at harmonics of the EC resonance and are usually considered fully absorbed after a single pass.

*e-mail: mads.senstius@physics.ox.ac.uk

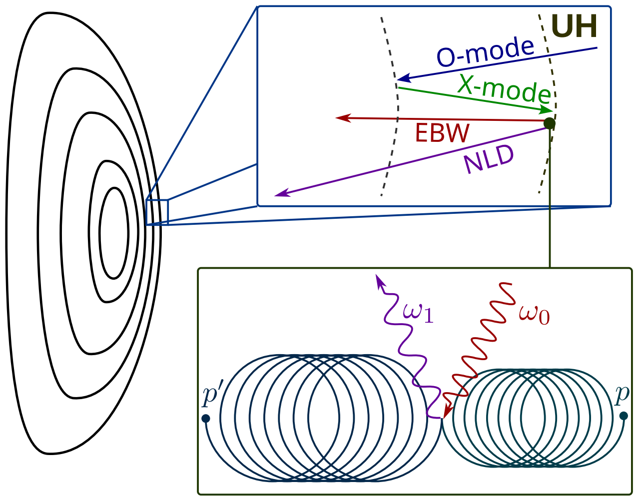


**Figure 1.** Illustration of the O-X-B mode coupling scheme and NLD as a two-wave-particle interaction. In MAST-U, O-X-B takes place in the edge of the plasma as indicated by the flux surfaces in left side of the figure. The O-X-B is sketched in the top right part of the figure; and injected O-mode beam couples to X-mode at the plasma cutoff, which couples linearly to an EBW at the UH layer and then turns around, propagating to higher density. At the UH layer, NLD can produce a daughter wave shifted in frequency by interacting with gyrating particles as indicated in the bottom right figure.

The EBWs cannot propagate in vacuum and can therefore not be excited by antennae outside a plasma to be injected into it. Instead, they can be coupled to via different mode coupling schemes. For MAST-U and STEP, the O-X-B scheme[6] is planned to be employed and it is illustrated in figure 1. For this, gyrotrons will inject beams polarized as O-mode, which may couple linearly to X-mode with high efficiency at the O-mode cutoff if aimed correctly. The X-mode waves continue beyond the O-mode cutoff but are reflected at the L-cutoff after which it propagates out to the UH layer. In the full electromagnetic kinetic model, the X-mode waves transition to electrostatic EBWs near the UH frequency. The EBWs will eventually become backward propagating, turning around once again and propagating towards the core of the devices where a harmonic of the EC resonance can be placed for the waves to be absorbed at.

## 2.2 Nonlinearities commonly associated with the upper hybrid (UH) layer

The turning point of the EBW is a caustic where the wave field amplifies and the group velocity decreases. Both of these effects make nonlinear wave interactions more likely to occur. A wave instability commonly associated with the UH layer is the parametric decay instability, which was studied for MAST-U parameters previously[3]. The parametric decay instability is a low order wave-wave instability where a large amplitude pump wave decays into two daughter waves, which satisfy the resonant selection rules $\omega_0 = \omega_1 + \omega_2$ and $\mathbf{k}_0 = \mathbf{k}_1 + \mathbf{k}_2$. The study focused on the injected X-mode wave at the UH layer, which couples to a lower hybrid wave and a correspondingly downshifted EBW. In addition to this, the study looked into stochastic electron heating where the large amplitude longitudinal field from the EBWs cause electron orbits to become chaotic and the electrons then absorb energy rapidly. The onset of both effects in PIC simulations were found to agree with expressions for thresholds found in past literature and the linear excitation of EBWs was found to scale poorly with injected power above the thresholds. However, it was not clear that these two effects were accountable for all of the nonlinear losses.

## 2.3 The nonlinear Landau damping resonance condition

Because of the plasma parameters at the UH layer in MAST-U, a nonlinear wave-particle interaction, which is higher order in the electric field, known as nonlinear Landau damping (NLD)[4, 7] is possible. This effect has also been called two-wave-particle scattering and is described as waves scattering on particles, producing a wave at a different frequency with the difference in energy and momentum being transferred to the particles. In the geometry of the PIC simulations in [3], all waves were propagating perfectly perpendicular to the magnetic field in a magnetized plasma without drifts, and the resonance condition for NLD can then be written as

$$\omega_0 - \omega_1 = r\omega_{c\sigma}, \tag{1}$$

where $r \in \mathbb{Z}$ is an integer and $r\omega_{c\sigma} = rq_\sigma B/(m_\sigma \gamma)$ is a harmonic of the cyclotron frequency, $q_\sigma$ and $m_\sigma$ are the charge and mass of particles of species $\sigma$, $B$ is the magnitude of the background magnetic field, $\gamma = \sqrt{1 + (p_\parallel^2 + p_\perp^2)/(m_\sigma c)^2}$ is the relativistic Lorentz factor with $c$ being the speed of light and $p_\parallel$ and $p_\perp$ being the parallel and perpendicular components of the momentum of the particles that resonate with this process. We note that equation (1) is the $k_\parallel = 0$ case of equation (1) in [4] if $\gamma = 1$. Although more complicated in reality, this process can be thought of as a three-wave interaction where one wave is the cyclotron motion of the particles of the plasma. In the context of O-X-B in MAST-U, the UH layer is found on the EBW branch between the second and third harmonic of the EC frequency, and NLD can therefore lead to the generation of EBWs downshifted by the EC frequency. For an $\omega_0/(2\pi) = 34.8$ GHz gyrotron pump wave in MAST-U, the resulting wave would be an $\omega_1/(2\pi) \approx 20$ GHz EBW which could still be absorbed at its EC resonance found in a different part of the plasma. In figure 2, the first three harmonics of the EC frequency are plotted for the low field side of an L-mode MAST-U plasma. A wave at $\omega_1$ has its fundamental EC resonance inside the plasma, but it is shifted from the second harmonic of $\omega_0$ by a considerable distance and into the high field side. Furthermore, the energy and momentum transfer to the electrons may lead to heating and current drive near the UH layer instead of at harmonics of the EC resonance. This may lead to a highly gyrotron power sensitive deposition profile.

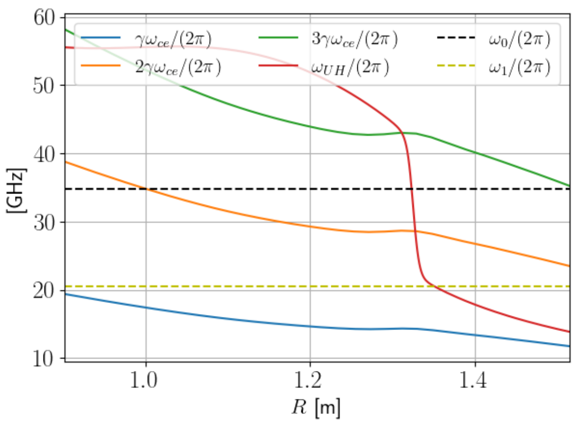


**Figure 2.** Locations of harmonics of the EC resonance in MAST-U along with the UH frequency. The plasma parameters are taken along the midplane in the low field side of the reactor. The pump wave is marked by the horizontal dashed black line which would couple to an EBW at the UH layer and be absorbed at the second harmonic EC resonance. The daughter wave is marked by the horizontal dashed yellow line, which reaches an EC harmonic at a different position on the high field side instead. Note that $\gamma\omega_{ce}$ corresponds to the nonrelativistic EC frequency.

## 3 Obtaining a dynamic equation

### 3.1 Derivation of the nonlinear dispersion relation

The EBW and NLD are kinetic phenomena and the starting point is therefore the Vlasov equation

$$\frac{\partial f_\sigma}{\partial t} + \frac{\mathbf{p}}{m_\sigma \gamma}\cdot\frac{\partial f_\sigma}{\partial \mathbf{x}} + q_\sigma\left[\mathbf{E} + \frac{\mathbf{p}}{m_\sigma\gamma}\times\mathbf{B}\right]\cdot\frac{\partial f_\sigma}{\partial \mathbf{p}} = 0, \quad (2)$$

where $f_\sigma$ is the particle distribution function, $\dfrac{\partial f_\sigma}{\partial \mathbf{x}}$ and $\dfrac{\partial f_\sigma}{\partial \mathbf{p}}$ are the gradients of the distribution function in position and momentum space, **E** is the electric field and **B** is the magnetic field. A relativistic description of NLD is not generally needed, however, the geometry of the PIC simulations in [3] require this. The simulations are 1D with all waves propagating perpendicular to the background magnetic field. With zero parallel wavenumber, the EC frequency is a singularity which turns out to be problematic even though $\omega_0 \neq \omega_{ce} \neq \omega_1$. In a relativistic model, the cyclotron frequency is modified by the Lorentz factor, causing the particles to resonate at a frequency which depends on where the particles are in momentum space. We then use a similar approach as has previously been explored in [4, 7, 8] and assume that the electric field is a superposition of electrostatic waves, which is valid for the EBWs and approximately so for X-mode near the UH layer. To conform to the 1D PIC simulations, we align all waves with the $x$-axis such that $\mathbf{E} = \sum_j E_j e^{i[k_j x - \omega_j t]}\hat{\mathbf{x}}$, where $\hat{\mathbf{x}}$ is the unit vector in the $x$-direction, and $E_{-j} = E_j^*$ with $\omega_{-j} = -\omega_j$, $k_{-j} = -k_j$. With this sum, we model the electric field as a superposition of some arbitrary number of waves. Each wave has an amplitude, $E_j$, a wavenumber, $k_j$, and a frequency, $\omega_j$, which are all referred to using the subscript $j$. Note that it is fairly straight forward to include propagation with a component of the wavevector parallel to the magnetic field and that this will not change later conclusions. We assume that there is no DC electric field. For the distribution function, we assume a similar superposition but allow for a background distribution, $f_\sigma = g_\sigma + \sum_j f_{\sigma,j} e^{i[k_j x - \omega_j t]}$ where $g_\sigma$ is the background distribution. Lastly, we assume that there are no oscillatory contributions to the magnetic field, $\mathbf{B} = B\hat{\mathbf{z}}$ where $\hat{\mathbf{z}}$ is the unit vector pointing in the $z$-direction. As done in past literature, we will for now assume that there is no position and time dependence other than the harmonic oscillations of the complex exponentials. Collecting terms that oscillate alike and going to cylindrical coordinates around the magnetic field lines in momentum space, a first order inhomogeneous differential equation is obtained for $f_{\sigma,j}$. It can be shown that the solution can be written as

$$f_{\sigma,j} = \frac{q_\sigma}{\omega_{c\sigma}} G_{\sigma,j}(\theta) \int^\theta G_{\sigma,j}(-\theta')\Bigg(E_j \cos(\theta')\frac{\partial g_\sigma}{\partial p_\perp} + \sum_{j'\neq j} E_{j-j'}\left[\cos(\theta')\frac{\partial f_{\sigma,j'}}{\partial p_\perp} - \frac{\sin(\theta')}{p_\perp}\frac{\partial f_{\sigma,j'}}{\partial \theta'}\right]\Bigg)d\theta' \quad (3)$$

$$G_{\sigma,j}(\theta) = \exp\left(i\frac{\omega_j\theta - \dfrac{p_\perp k_j}{m_\sigma\gamma}\sin(\theta)}{\omega_{c\sigma}}\right) = e^{i[a_j\theta - \rho_L k_j \sin(\theta)]}, \quad (4)$$

where subscripts like in $E_{j-j'}$ refer to the component that oscillates like the difference in frequency and wavenumber of indices $j$ and $j'$, $a_j$ is a normalized frequency and $\rho_L$ is the Larmor radius. The right hand side of $f_{\sigma,j}$ contains $f_{\sigma,j'}$ which can be substituted in recursively to generate terms with more products of the electric field amplitudes. Note that the solution to $f_{\sigma,j}$ does not contain itself on the right hand side as there is no zero frequency electric field. This is inserted into Gauss' equation with the density of species $\sigma$ factored out of the distribution functions such that

$$ikE_j = \sum_\sigma \frac{m_\sigma \omega_{p\sigma}^2}{q_\sigma}\int f_{\sigma,j} d\mathbf{p}, \quad (5)$$

where $\omega_{p\sigma} = \sqrt{q_\sigma^2 n_\sigma/(\epsilon_0 m_\sigma)}$ is the plasma frequency of species $\sigma$, $n_\sigma$ is the density of the species, $\epsilon_0$ is the vacuum permittivity and the integral is over all of momentum space. We now make the assumption that we are considering a background plasma that is perturbed by electrostatic waves with amplitudes such that $E_j = \sum_{l=1}^\infty E_j^{(l)}$, $E_j^{(l)} \gg E_{j'}^{(l+1)}$ and $E_j^{(l)} E_{j'}^{(l')} \sim E_{j''}^{(l+l')}$, where $j = j'$ and $l = l'$ are also valid. That is, there are increasingly small nonlinear corrections and the order of these corrections add up when quantities are multiplied. Inserting the expression for $f_{\sigma,j}$, we get to first order in the electric field

$$ikE_j^{(1)} = \sum_\sigma \frac{m_\sigma \omega_{p\sigma}^2}{\omega_{c\sigma}} E_j^{(1)} \int G_{\sigma,j}(\theta) \times \int^\theta G_{\sigma,j}(-\theta')\cos(\theta')\frac{\partial g_\sigma}{\partial p_\perp} d\theta' d\mathbf{p}. \quad (6)$$

The most obvious choice for $g_\sigma$ is a normalized Maxwell-Jüttner distribution, however, it can be shown from our Vlasov equation that the background distribution function must be independent of $\theta$. Using the Bessel identity $e^{i\rho_L k \sin(\theta)} = \sum_{r=-\infty}^{\infty} J_r(\rho_L k)e^{ir\theta}$, the $\theta'$ integral can be solved and calculating the $2\pi$ average over $\theta$, since we are going to integrate over $2\pi$ in momentum space later, we get the linear dispersion relation on a more compact form

$$\varepsilon(\omega_j, k_j)E_j^{(1)} = 0 \tag{7}$$

$$\varepsilon(\omega_j, k_j) = k_j^2 + \sum_\sigma \int \frac{m_\sigma \omega_{p\sigma}^2}{\rho_L} \frac{\partial g_\sigma}{\partial p_\perp} \sum_{r=-\infty}^{\infty} \frac{r J_r(\rho_L k_j)^2}{\omega_j - r\omega_{c\sigma}} d\mathbf{p}, \tag{8}$$

where $J_r(\rho_L k)$ is the $r^{\text{th}}$ Bessel function of the first kind. The interpretation is that only waves that satisfy $\varepsilon(\omega_j, k_j) = 0$ can have a nonzero amplitude to first order. To second order, we get the same linear term along with a three-wave coupling term which after several manipulations can be written as

$$\varepsilon(\omega_j, k_j)E_j^{(2)} = \sum_{j'\neq\varnothing} M_{j,j'} E_{j-j'}^{(1)} E_{j'}^{(1)} \tag{9}$$

$$M_{j,j'} = i \sum_{\sigma,r_1,r_2,r_3} q_\sigma m_\sigma \omega_{p\sigma}^2 \frac{k_j}{k_{j'}} \int \frac{J_\varrho(\rho_L k_j)}{\omega_j - \varrho\omega_{c\sigma}} \left[ \frac{r_3}{\rho_L k_j} J_{r_3}(\rho_L k_j) \frac{\partial}{\partial p_\perp} + \frac{r_2 - r_1}{p_\perp} J'_{r_3}(\rho_L k_j) \right] \left[ \frac{1}{\rho_L} \frac{r_1 J_{r_1}(\rho_L k_{j'}) J_{r_2}(\rho_L k_{j'})}{\omega_{j'} - r_1\omega_{c\sigma}} \frac{\partial g_\sigma}{\partial p_\perp} \right] d\mathbf{p}, \tag{10}$$

where $\varrho = r_3 - r_2 + r_1$ and index $\varnothing$ referring to a zero frequency and wavenumber wave. We note that this is a crude form of the coupling coefficient, which may be simplified. However, this form contains the features needed in our later analysis. Importantly, the second order field $E_j^{(2)}$ can be nonzero for $\varepsilon(\omega_j, k_j) \neq 0$ which we refer to as a virtual wave. Finally to third order, we again get a linear term and a three-wave term but we now also get a four-wave term which may be written as

$$\varepsilon(\omega_j, k_j)E_j^{(3)} = \sum_{j'\neq\varnothing} M_{j,j'} \left( E_{j-j'}^{(1)} E_{j'}^{(2)} + E_{j-j'}^{(2)} E_{j'}^{(1)} \right) + \sum_{j'\neq\varnothing, j''\neq\varnothing} L_{j,j',j''} E_{j-j'}^{(1)} E_{j'-j''}^{(1)} E_{j''}^{(1)}. \tag{11}$$

Although the four-wave coupling coefficient can also contribute to NLD, we will neglect it here and set $L_{j,j',j''} = 0$. Instead, we focus on the three-wave coupling with the virtual waves. We will justify this in section 4. Substituting $E_j^{(2)}$ from the second order equation into the third order equation, manipulating the sum indices and adding the 3 orders together assuming $E_j^{(1)} + E_j^{(2)} + E_j^{(3)} \approx E_j \approx E_j^{(1)}$, we get

$$\varepsilon(\omega_j, k_j)E_j = \sum_{j'\neq\varnothing} M_{j,j'} E_{j-j'} E_{j'} + \sum_{j',j''} M_{j',j''} \frac{M_{j,j'} + M_{j,j-j'}}{\varepsilon(\omega_{j'}, k_{j'})} E_{j-j'} E_{j'-j''} E_{j''}, \tag{12}$$

where $j' \neq \varnothing$ and $j'' \neq \varnothing$ for the first term of the numerator on the right hand side while $j' \neq j$ for the other term. We note that substituting the second order fields is only valid if they are virtual waves that do not satisfy the linear dispersion relation.

### 3.2 The weakly inhomogeneous wave equation

The equations so far are assuming that the background plasma is infinite, time stationary and homogeneous but this assumption is not applicable for the MAST-U plasma. In papers such as [4, 7], it is assumed that the linear part of the dielectric tensor elements, i.e. the left hand side of equation (12), may give rise to new terms when introducing the inhomogeneity but that corrections to the remaining nonlinear terms are neglected as they would be even higher order terms. Replacing the left hand side with a general nonlocal linear dispersion relation in a time stationary medium depending only on the $x$-position whilst keeping the right hand side but evaluating everything at the $x$-position, we can write

$$\int_{-\infty}^{\infty} \mathcal{L}\left(\omega_j, x - x', \frac{x + x'}{2}\right) E_{j,tot}(x')dx' = \mathcal{N}_j(x), \tag{13}$$

where $\mathcal{L}$ is a linear integration kernel, $E_{j,tot}(x, t)$ is the wave electric field containing also its phase component and $\mathcal{N}_j$ contains all the nonlinear contributions along with phase components as well. We assume that nonlocal effects are weak, i.e. $\mathcal{L}$ is sharply peaked in $x - x'$, and that there is a only a weak dependence on $x + x'$, so we can apply a WKB procedure similar to [9]. To first order in the WKB expansion parameter $1/(kL)$, $L$ being the length scale over which a wave experiences a changing medium, the dynamical equation for the electric field amplitude can be written as

$$\left[ \varepsilon_j - i\frac{\partial\varepsilon_j}{\partial k_j}\frac{\partial}{\partial x} - \frac{i}{2}\frac{\partial^2\varepsilon_j}{\partial k_j \partial x} \right] E_j = \mathcal{N}_j e^{-i[k_j x - \omega_j t]}, \tag{14}$$

where we have suppressed all explicit $x$-dependence and $\varepsilon_j$ is short-hand notation for $\varepsilon(\omega_j, k_j)$ evaluated for parameters at the $x$-position.

## 4 Application to MAST-U

### 4.1 Dynamical equation in a two-wave system

We now apply this formula to a two-wave system consisting of a pump wave $(\omega_0, k_0)$ and a daughter wave $(\omega_1, k_1)$, as well as the complex conjugate waves. The pump wave is the gyrotron wave with $\omega_0 \approx \omega_{UH} = \sqrt{\gamma^2\omega_{ce}^2 + \omega_{pe}^2} > 2\gamma\omega_{ce}$. The daughter wave is also in the electron frequency range and contributions from much slower ion dynamics are neglected. We assume that the waves satisfy the real part of the dispersion and the linear damping of waves is then accounted for by the $\varepsilon_j E_j = \text{Im}(\varepsilon_j)E_j$ term of the dynamical equations for the waves. In principle, many interactions are possible, but we are assuming that only

$E_{\pm 0}$ and $E_{\pm 1}$ exist to first order. The dielectric tensor elements are complicated to evaluate numerically, in particular because some elements must be evaluated at the cyclotron frequency. It may be done using an approach like in [10], however, this is outside the scope of the present paper. Inspecting instead the quadratic coupling coefficient $M_{j,j'}$ analytically, we see that there are poles in momentum space whenever either of $\omega_j, \omega_{j'}$ are an integer times the relativistic cyclotron frequency. Whilst the pump and daughter waves are assumed to satisfy the linear dispersion relation, the virtual waves need only exist to second order and should not satisfy the dispersion relation. For this reason, virtual waves with frequencies close to multiples of $\gamma\omega_{ce}$ should produce the strongest coupling. We therefore assume $\omega_0 - \omega_1 = -\gamma\omega_{ce} = \gamma|\omega_{ce}|$, which is the NLD resonance condition. The other third order term which was neglected earlier, $L_{j,j',j''}$, is not expected to contribute as strongly to this effect since none of the 4 interacting waves can be virtual waves near cyclotron harmonics. The double sum in equation (12) can then be handled using a search algorithm. We note that upshifted waves at $\omega_0 + \gamma|\omega_{ce}|$ may also contribute in a way similar to $\omega_1$ but no EBWs satisfy the dispersion relation at that frequency for the parameters used in [3], so we neglect these waves here. Typically, EBWs do not propagate at the upshifted frequency when the pump frequency is very close to the UH frequency, and an EBW daughter wave downshifted by the EC frequency is only possible when $\omega_0 > 2\gamma|\omega_{ce}|$. All in all, we get the following dynamical equation for wave 1

$$\frac{\partial E_1}{\partial x} = \left(\frac{\partial \varepsilon_1}{\partial k_1}\right)^{-1}\left[i\frac{(M_{1-0,-0} + M_{1-0,1})(M_{1,1-0} + M_{1,0})}{\varepsilon(\gamma\omega_{ce}, k_1 - k_0)}|E_0|^2 + iM_{1,1}\frac{(M_{\varnothing,-0} + M_{\varnothing,0})|E_0|^2 + (M_{\varnothing,-1} + M_{\varnothing,1})|E_1|^2}{\varepsilon_\varnothing} - i\varepsilon_1 - \frac{1}{2}\frac{\partial^2 \varepsilon_1}{\partial x \partial k_1}\right]E_1. \quad (15)$$

The First term on the right hand side is the term that we attribute to NLD where a virtual wave at the cyclotron frequency gives rise to the NLD resonance condition. The second term in this expression is the coupling to zero frequency and wavenumber structures, which we will not explore further in this study. The remaining terms are remnants of the weakly inhomogeneous corrections to the linear dispersion relation. An entirely analogous expression is obtained for $E_0$ but we leave it out here for brevity.

## 4.2 Trouble in wave trajectories

The trajectory of the pump wave in the 1D PIC simulations in [3] is shown in $(x, k)$-space in figure 3 along with the wavenumber of the daughter wave as well as the difference in wavenumber, corresponding to that of the virtual wave. To generate the part of $k_0$ corresponding to X-mode, we have added a term to the linear dispersion relation associated with the electromagnetic dispersion relation as also found in [11]. This modification affects the low $k_0$ part which then behaves like cold X-mode would. Firstly, it can be seen that the turning point of the pump wave is found

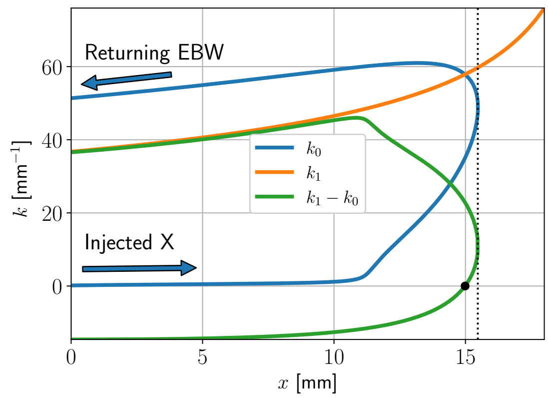


**Figure 3.** Wavenumbers of a pump wave, $k_0$, and a daughter wave, $k_1$, as well as the difference in the vicinity of the UH layer for a 1D geometry similar to the PIC simulations in [3]. The point where $\omega_0 = \omega_{UH}$ is marked by the dotted vertical line, the turning point of the pump wave is marked by the dashed vertical line and the point where $(k_1 - k_0) = 0$ is marked by a circle. These points are problematic within this type of framework.

beyond $\omega_0 = \omega_{UH}$. This happens because the UH layer is found between the second and third harmonic of the EC resonance. The turning point results in a fold type caustic and is a well known problem of the WKB approximation because the lengthscale that the wave changes over vanishes when the slope of the $(x, k)$-trajectory diverges. In our equations, this problem manifests itself in the $\partial\varepsilon/\partial k$ which goes through zero at turning points, leading to division by zero. Consequently, the linear part of the wave equation for the pump wave causes the amplitude to diverge and the NLD term in the equation for $E_1$ therefore also diverges. There are ways to deal with this problem. If it is assumed that the pump wave is undepleted, then its amplitude profile can instead be obtained by alternative models such as metaplectic geometric optics[12, 13]. This should be sufficient in order to determine a threshold provided that the daughter wave does not also encounter a turning point.

A more severe problem turns out to be the point where the difference in wavenumbers $(k_1 - k_0) \to 0$. This is problematic for several reasons. The most obvious issue is that the point violates the WKB assumption as the expansion parameter, $1/(kL)$, diverges for the virtual wave. However, it can be argued that the virtual wave was factored out and does not really appear in the equations that the WKB approximation was applied to. Another issue is that $\varepsilon(\omega, 0) = 0$, which means that the substitution of $E_j^{(2)}$ into the NLD coupling becomes invalid as the left hand side of equation (9) then vanishes and $E_j^{(2)}$ diverges in this limit. We further investigate this issue by checking if the limit of the coupling coefficent at $(k_1 - k_0) \to 0$ is finite or not. To do this, we use the series form of the Bessel function $J_r(x) = \sum_{j=0}^{\infty} \frac{(-1)^j}{j!(j+r)!}\left(\frac{x}{2}\right)^{2j+r}$ when $r \in \mathbb{N}^0$ and $J_{-r}(x) = (-1)^r J_r(x)$ for negative integers of $r$. As $k_1 - k_0 \to 0$, the leading term in the linear dispersion relation given by equation (8) goes as $\varepsilon(\omega_{ce}, k_1 - k_0) \sim (k_1 - k_0)^2$. Similarly, from equation (10) we get $M_{1-0,j} \sim (k_1 - k_0)^1$ and $M_{j,1-0} \sim (k_1 - k_0)^0$. This means that the total NLD coupling coefficient in equation (15) goes as $\sim (k_1 - k_0)^{-1}$ when $(k_1 - k_0) \to 0$. One might argue that the terms with poles near the EC resonance dominate, however, the poles lead to finite contributions and the coupling will diverge when the difference in wavenumber is sufficiently small. If we instead of substituting the homogeneous second order field into the third order equation used the weakly inhomogeneous wave equation to get a set of coupled equations for $E_0, E_1$ and $E^{(2)}_{1-0}$, the results would still diverge. Mathematically, the problem is that $\left.\frac{\partial\varepsilon(\omega, k)}{\partial k}\right|_{k=0} = 0$ so the $(k_1 - k_0) = 0$ point is a caustic for the virtual wave. As discussed earlier, the WKB approximation is not valid here. Unlike at the turning point for $E_0$, metaplectic geometrical optics cannot reconstruct $E^{(2)}_{1-0}$ properly in this point because the virtual wave has nonlinear contributions which presently has not yet been incorporated into metaplectic geometrical optics.

## 5 Discussion and conclusion

We have presented the typical framework for modeling weakly nonlinear wave dynamics of microwaves in fusion plasmas and applied it to NLD in MAST-U with the intent of studying the impact of NLD on the coupling from X-mode to an EBW at the UH layer in 1D PIC simulations. The problem turns out to be complicated for a number of reasons. Firstly, the derivation had to be relativistic even if the interactions occur in the edge of the plasma where the electron temperature is so low that relativistic corrections would normally be disregarded. This is because the simulation geometry would otherwise lead to a singularity at the EC frequency. A simple fix could have otherwise been to allow all waves to propagate with a small wavenumber parallel to the magnetic field, but this should be equivalent in the limit of no parallel wavenumber where it diverges. This seems to imply that an arbitrarily strong coupling could be obtained by picking the parallel wavenumber intentionally in a non-relativistic model. Physically, the difference is that the entire distribution function can resonate with the EC frequency at the same time in a non-relativistic model but the frequency becomes dependent on the momentum of the particles in the relativistic model, thereby avoiding a singularity.

Having dealt with this problem, other issues arise in the way that weakly inhomogeneous media are typically modeled with the WKB approximation. Two points in the vicinity of the UH layer are identified as problematic. One is the caustic at the EBW turning point and the other is the point where the difference in wavenumber between the injected pump wave and an EBW downshifted by the EC frequency vanishes. Whilst methods exist to handle the caustic, the other point requires an even more careful treatment. Simply adding inhomogeneous corrections to the nonlinear part of the dispersion relation the same way that the linear part was modified will not solve the model as the small WKB parameter diverges for the virtual wave. An approach not relying on WKB might be necessary, however, the tensor elements would likely be much more complicated. Ultimately, a large part of the region of interest for nonlinear effects like NLD cannot be treated with standard methods and attempting to do so might falsely indicate a devastating impact of NLD on O-X-B in MAST-U.

It is important to mention here that the existence of the point where $(k_1 - k_0) = 0$ is not a coincidence of the geometry where waves propagate perpendicular to the magnetic field. Due to the large range of wavenumbers that the pump wave attains during the coupling to EBWs as indicated in figure 3, this is likely to occur somewhere during O-X-B. Although the divergent behavior is unphysical a strong coupling could still occur in such points. A strong coupling could lead to modifications to the current drive profiles, generating a current also at the UH layer and at the EC resonance of the daughter wave.

## 6 acknowledgments

The work presented here is supported by the Carlsberg Foundation, grant CF23-0181, the Novo Nordisk Foundation, NNF22OC0076017, and the Lucy Halsall Fund Grant.

## References

[1] V. Shevchenko *et al*, Nuclear Fusion **50**, 022004 (2010), http://dx.doi.org/10.1088/0029-5515/50/2/022004

[2] S. Freethy *et al*, EPJ Web of Conferences **277**, 04001 (2023), https://doi.org/10.1051/epjconf/202327704001

[3] M. G. Senstius *et al*, EPJ Web of Conferences **277**, 01009 (2023), https://doi.org/10.1051/epjconf/202327701009

[4] M. Porkolab and R. P. H. Chang, The Physics of Fluids **15**, 283 (1972), https://doi.org/10.1063/1.1693906

[5] R. P. H. Chang and M. Porkolab, Physical Review Letters **25**, 1262, (1970), https://doi.org/10.1103/PhysRevLett.25.1262

[6] J. Preinhaelter and V. kopecký, J. Plasma Physics, **10**, 1-12, (1973), https://doi.org/10.1017/S0022377800007649

[7] R. Sugaya, Physics of Plasmas, **10**, 10, 3939 (2003), https://doi.org/10.1063/1.1612498

[8] R. E. Aamodt, Physical Review, **138**, 1A 45 (1965), https://doi.org/10.1103/PhysRev.138.A45

[9] H. L. Berk and D. Pfirsch, J. Math. Phys., **21**, 2054 (1980), https://doi.org/10.1063/1.524716

[10] S. S. Pavlov and F. Castejon, Nuclear Fusion, **58**, 126030 (2018), https://doi.org/10.1088/1741-4326/aae6f0

[11] S. K. Hansen *et al*, Phys. Plasmas, **30**, 042103 (2023), https://doi.org/10.1063/5.0138249

[12] N. A. Lopez and I. Y. Dodin, J. Opt. **23**, 025601 (2021), https://doi.org/10.1088/2040-8986/abd1ce

[13] R. H. Marholt, M. G. Senstius and S. K. Nielsen, Physical Review E, **110** 025208, https://doi.org/10.1103/PhysRevE.110.025208